Mestrado Integrado em Medicina Dentária

Faculdade de Medicina da Universidade de Coimbra

Avaliação da contração de polimerização com recurso a redes de Bragg gravadas em fibra óptica: estudo piloto

Polymerization shrinkage evaluation using fiber Bragg grating sensors: a pilot study

Miriam Leonor Rodrigues Rebelo

Orientador: Prof. Doutor João Carlos Ramos

Co-orientadora: Dra. Alexandra Vinagre

Coimbra, 2012

Avaliação da contração de polimerização com recurso a redes de Bragg gravadas em fibra óptica: estudo piloto

Polymerization shrinkage evaluation using fiber Bragg grating sensors: a pilot study

M. Rebelo, A. Vinagre, J. C. Ramos

Department of Dentistry, Faculty of Medicine, University of Coimbra
Av. Bissaya Barreto, Blocos de Celas
3000-075 Coimbra
Portugal

E-mail: miriamrebelo@hotmail.com

Abstract

Introduction: due to their excellent aesthetic properties and to the improvement of some mechanical properties, the composites have been acquiring increasing importance in the context of oral rehabilitation. There are, however, some disadvantages that may compromise their clinical success, such as polymerization shrinkage, which could be associated to contraction stress transferred to the tooth, leading to cusp deflection and/or enamel microcracks. On the other hand, stress at the tooth-composite interface has the potential to cause adhesive failure, leading to post-operative sensitivity, microleakage, recurrent caries, and ultimately, to pulp inflammation.

Objectives: The aim of this work was to make a pilot study regarding the capability of optical fiber Bragg grating (FBG) sensors to evaluate the linear polymerization shrinkage of composite resins.

Materials and methods: Two different composite resins (SDR™ and Esthet• X® HD – Dentsply DeTrey, Konstanz, Germany) were placed in plastic molds crossed by a fiber Bragg grating sensor and light-cured by a LED unit (Bluephase®, Ivoclar Vivadent, Lichtenstein). Strain in με was plotted as a function of time (seconds), obtaining a representative curve. Besides linear shrinkage evaluation, additional measurements were made concerning the

temperature rise induced on the FBG sensor solely due to the LED light curing irradiation and for thermal characterization of both composite resins during light-curing process.

Results: it was observed an initial expansion either due to thermal absorption of light curing unit either from the exothermic reaction of composite polymerization immediately followed by linear contraction, which reached 0,43% to Esthet• X® HD and 0,42% to SDR™.

Conclusions: The optical fiber Bragg grating sensors can be used to evaluate linear polymerization shrinkage of dental composites with clear advantages to assess the evolution of composite shrinkage in real time during all polymerization process.

Keywords: polymerization shrinkage, composite resin, optical fiber sensor, fiber Bragg grating

Resumo:

Introdução: devido às suas excelentes propriedades estéticas e à melhoria das suas propriedades mecânicas, as resinas compostas têm vindo a conquistar um papel progressivamente crescente no âmbito da reabilitação oral. Contudo, de entre algumas das suas desvantagens inerentes, a contração de polimerização assume um papel crucial pelas consequências que pode originar como a deflexão cuspídea, propagação de microfracturas e ruptura da interface adesiva da restauração, potenciando a presença de fendas marginais e consequente microinfiltração, sensibilidade pós-operatória, recidiva de cárie e, em última instância, de patologia pulpar.

Objectivos: realizar um estudo piloto sobre a capacidade de avaliação da contração de polimerização linear de resinas compostas com recurso a redes de Bragg gravadas em fibra óptica (FBG).

Materiais e métodos: introduziu-se uma rede de Bragg num molde de plástico, que posteriormente se preencheu com duas resinas compostas (SDR™ e Esthet• X® HD – Dentsply DeTrey, Konstanz, Germany) colocadas ao redor da fibra, procedendo-se à sua fotopolimerização com um fotopolimerizador de LEDs (Bluephase®, Ivoclar Vivadent, Lichtenstein). A força da contração, medida em με, foi traçada em função do tempo (em segundos), obtendo uma curva representativa da contração linear. Para além da contração, foram registadas as variações de temperatura provocadas somente pela irradiação do fotopolimerizador de LEDs e durante a polimerização das resinas compostas.

Resultados: foi possível observar uma ligeira expansão inicial das resinas compostas imediatamente seguida por contração linear que atingiu valores de 0,43% para o Esthet• X® HD e 0,42% para o SDR™.

Conclusões: O uso de FBG para avaliação da contração de polimerização linear das resinas compostas é um método viável com vantagens claras na monitorização em tempo real de todo o processo de polimerização.

Introduction

Volumetric shrinkage of composite resins (1-6%) and inherent contraction stress arising during the polymerization reaction are significant drawbacks of these materials [1-4]. Shrinkage stress transferred to the tooth may lead cusp deflection or enamel microcracks, whereas stress at the tooth-composite interface has the potential to cause adhesive failure, leading to post-operative sensitivity, microleakage, marginal discoloration, recurrent caries and ultimately, to pulp inflammation [1, 4-16]. An early clinical manifestation of the harmful nature of these tensions of contraction is the appearance of white lines along the cavo-surface margins of restorations. With time, this margins decline becomes evident with the appearance of cracks and interfacial pigmentation [1].

Different approaches have been proposed to reduce polymerization shrinkage of composite resins, including incremental placement techniques, the development of “soft-start like” polymerization techniques, the use of low E-modulus intermediate layers and alternative chemical formulations of dimethacrylate-based composite resins [2, 3, 14, 17]. One of the most obvious strategy for dealing with shrinkage stresses is eliminating or reducing polymerization shrinkage [4]. More recently, some entitled “low-shrinkage” composite resins were developed to reduce either polymerization shrinkage and/or stress. This class of materials were introduced based on different approaches such as: incorporating high levels of fillers; modifying the monomeric composition of the resin matrix by reducing the incorporation of low-molecular weight dimethacrylates, as a positive correlation can be found between its content and the amount of carbon double bonds per unit volume [18]; introducing non-silanized filler or introducing an alternative chemical composition to dimethacrylate resins [15, 19], like cationic ring-opening curing systems presented in siloranes [13, 17, 20, 21] or by adding a polymerization modulator [14, 17, 19]. Nevertheless, none of them has scientifically proved to be clinically superior to Bis-GMA based composites [1-3, 22, 23].

Furthermore, the magnitude of composite resins shrinkage depends also on the methodology used to measure it. Shrinkage of dental composites has been broadly evaluated through many methods, such as dilatometers [3, 22, 24-27], bonded disk technique [9, 20, 24-27], electrical resistance strain gauges [24, 27-29], linometer [24, 27, 30]; FEA (Finite Element Analysis) [2, 16, 24, 27, 31-33]; CMM (Coordinate Measuring Machines) [23], OCT (Optical Coherence Tomography) [23, 31], optic Fizeau interferometer [34], gas pycnometer [35, 36], by video images like AcuVol™ or Drop Shap Analysis System Model [37-39], X-ray microtomography [24, 37, 40-42], wall-to-wall shrinkage [27], theometer pycnometer, thermo-mechanical analyzer [35] and fiber Bragg grating (FBG) sensors [43-46].

Most of the times, the magnitude of stress transferred to the tooth or adhesive interface is more important than polymerization shrinkage itself. Besides, it is important to

emphasize that shrinkage stress is not a material property, but rather a result of a multitude combination of factors [2, 47]. Several methods used to evaluate shrinkage stress can be found in the literature as ring slitting method [24], Finite Element Analysis [2, 16, 24, 31-33], force transducers [24], Bioman [24, 48], stress strain analyser [22, 49], photo-elastic analysis [2], crack propagation [48] , extensometers [24], universal testing machines [29, 48, 49], tensilometer [2, 27] and radial-cut-cylinder-bending method [50].

Fiber optical sensors are currently being used in biomedical applications due to its reduced dimensions, chemical inertness, high sensitivity, compatibility [43, 46], immunity to electromagnetic interference [45], resolution and the ease to use in most applications [44]. Its major advantage is the possibility for accurate real-time monitoring strains. Additionally, standard fiber Bragg grating (FBG) sensors can be used to monitor temperature and strain [43, 44, 46].

The objective of this work was to make a pilot study regarding the capability of optical fiber Bragg grating (FBG) sensors to evaluate the linear polymerization shrinkage of composite resins.

Materials and methods

In this research study, fiber Bragg grating (FBG) sensors, FiberCore PS 1250/1500 produced by the Instituto de Telecomunicações (Pólo de Aveiro, Portugal) were used to assess linear polymerization shrinkage of two composite resins: SDR™ and Esthet• X® HD (Dentsply DeTrey, Konstanz, Germany) (Table I).

Table I: Materials studied, manufacturers, composition and batch numbers.

Composite	Manufacturer	Type	Resin Matrix	Filler	Batch no.
SDR™	Dentsply DeTrey	Microhybrid	Modified UDMA EBPADMA TEGDMA	Ba-Al-F-B-Si-glass Sr-Al-F-Si-glass (68 wt %., 45 vol %)	1201231
Esthet•X® *HD*	Dentsply DeTrey	Microhybrid	Bis-GMA adduct Bis-EMA adduct TEGDMA	Ba-F-Al-B-Si-glass Nanofiller sílica (77wt%; 60 vol%)	1112302

Bis-GMA (Bisphenol A dimethacrylate); Bis-EMA (Bisphenol A polyethylene glycol diether dimethacrylate); UDMA (urethane dimethacrylate); TEGDMA (Triethyleneglycol dimethacrylate); EBPADMA (ethoxylated Bisphenol A dimethacrylate)

The FBG sensor is inscribed into a photosensitive single mode optical fiber comprising a core with 9,6 µm diameter, made of silica doped with germanium and boron, surrounded by a cladding layer with 125 µm diameter, made of high purity silica. To provide mechanical resistance, the fiber was coated with a polymer, consisting in a urethane acrylate coating. This whole procedure results in an overall fiber diameter of 250 µm [51].

The FBG sensors used in this study were written in a standard single mode photosensitive fiber (FiberCore PS1250/1500) with a UV light (248 nm) with a KrF excimer laser, using the phase mask system [46, 51]. The region where the fiber has a protective coating has been removed to allow recording FBG. The optical sensing interrogator used was the sm125-500 Micron Optics (Micron Optics Inc, Atlanta, USA) with a wavelength resolution of 1 pm. Laser emitted by sm125-500 has a wavelength between 1510-1590 nm.

A fiber Bragg grating sensor is a periodic modulation of the refractive index inscribed in the fiber core of a single-mode optical fiber along a small length, with 4 mm in this study. This periodic modulation of refractive index in the fiber core acts as a selective filter for the

wavelength that satisfies the Bragg condition. When the fiber that contains the FBG is illuminated by a broadband light source, the wavelength of propagation mode that satisfies the Bragg condition is reflected, being all the others transmitted. When that condition is not satisfied, the components become progressively out of phase, nullifying themselves [46, 51].

The Bragg condition is given by: $\lambda_{B=} 2\Lambda n_{eff}$

Where λ_B is the Bragg wavelength, Λ is the periodic modulation of the refractive index and n_{eff} the effective refractive index of the fiber core [46, 51]. The effective refractive index, as well as the periodic spacing between the grating planes, will be affected by changes in strain and/or temperature which will amend the center wavelength of light back reflected from a Bragg grating. Using the first equation, the shift in the Bragg grating center wavelength due to strain and temperature changes is given by:

$$\Delta\lambda_B = 2\left(\Lambda\frac{\partial n}{\partial l} + n\frac{\partial\Lambda}{\partial l}\right)\Delta l + 2\left(\Lambda\frac{\partial n}{\partial T} + n\frac{\partial\Lambda}{\partial T}\right)\Delta T = \Delta\lambda_{Bl} + \Delta\lambda_{BT}$$

Where $\Delta\lambda_{Bl}$ is the strain-induced wavelength shift $\left(\Lambda\frac{\partial n}{\partial l} + n\frac{\partial\Lambda}{\partial l}\right)$ and $\Delta\lambda_{BT}$ is the temperature-induced wavelength shift ; these values are constants $\left(\Lambda\frac{\partial n}{\partial T} + n\frac{\partial\Lambda}{\partial T}\right)$: the strain and temperature sensitivities of the FBG sensors are 0,00115 nm/με and 0,0084 nm/ºC, what means that correspond respectively to $\Delta\lambda_{Bl}$ and to $\Delta\lambda_{BT}$.

Induced strain of the FBG structure changes its refractive index and, consequently its wavelength due to two main events. First, the refractive index of the fiber is modified while grating is also structurally deformed when the mechanical stress acts through the silica tensor components. Second, any temperature variation induces changes in the refractive index due to the thermo-optic effect causing a thermal expansion or contraction of the structure. Hence, in order to acquire real-time strain data using FBG sensors, separate temperature monitoring is required. For this reason, the first procedure performed in this study was related to the measurement of the temperature rise induced on the FBG sensor due to the LED (Light Emitting Diode) light curing irradiation (Bluephase®, Ivoclar Vivadent, Lichtenstein). For this, the FBG sensor was inserted into a needle and photo-activation was carried out with a selected irradiation protocol, consisting in two periods of 30 seconds irradiation time at low mode intensity, separated by 5 minutes (figure 1).

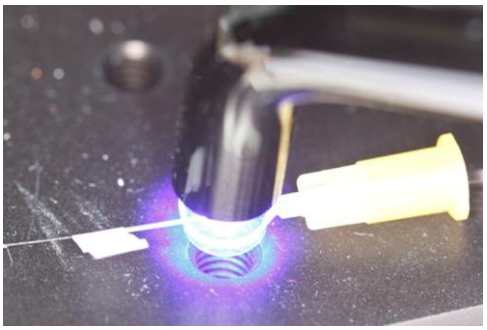

Figure 1: Measurement of the temperature rise induced on the FBG sensor due to the LED light curing irradiation.

This curing protocol was applied in all subsequent necessary measurements, both the temperature assessment induced by composite polymerization and for linear strain evaluation of composite resins during its polymerization.

For thermal characterization of both composite resins during light-curing process, a FBG sensor was placed into a needle crossing a plastic mold with 7,5 mm diameter and 2,5 mm thickness (figure 2a), containing the 4 mm inscription FBG sensor. The mold has been filled with composite resin (figure 2b) and light activated according to the selected irradiation protocol with the light tip positioned 3 mm above the sample.

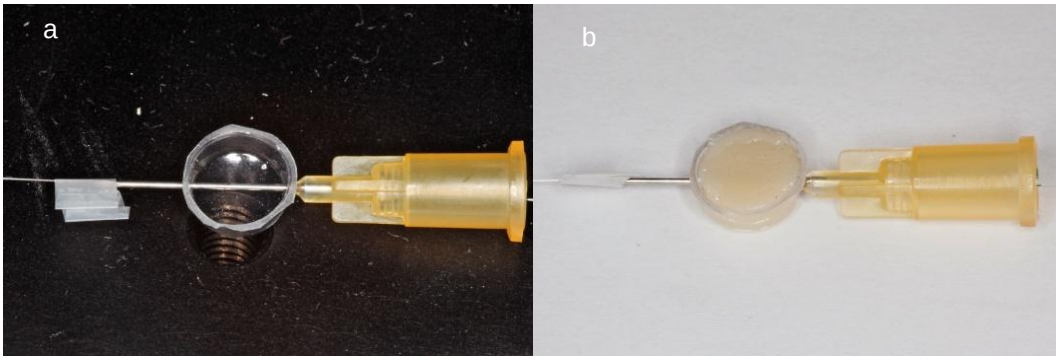

Figure 2: Measurement of composite resin temperature respecting the selected irradiation protocol: a) plastic mold with the needle that contains FBG; b) plastic mold with composite resin.

Finally, for composite shrinkage evaluation, the needle was removed and the composite carefully introduced into the mold and around the fiber surface, avoiding defects such as air bubbles (figure 3a, 3b and 3c). Light curing was performed as described above (figure 4a and 4b).

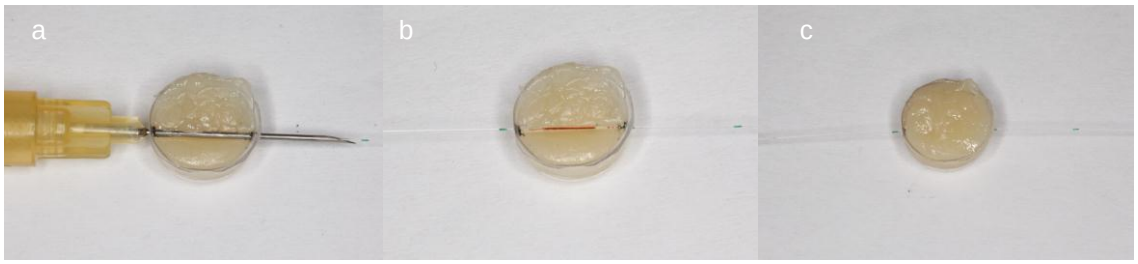

Figure 3a, 3b and 3c: Composite insertion into to the mold and around fiber.

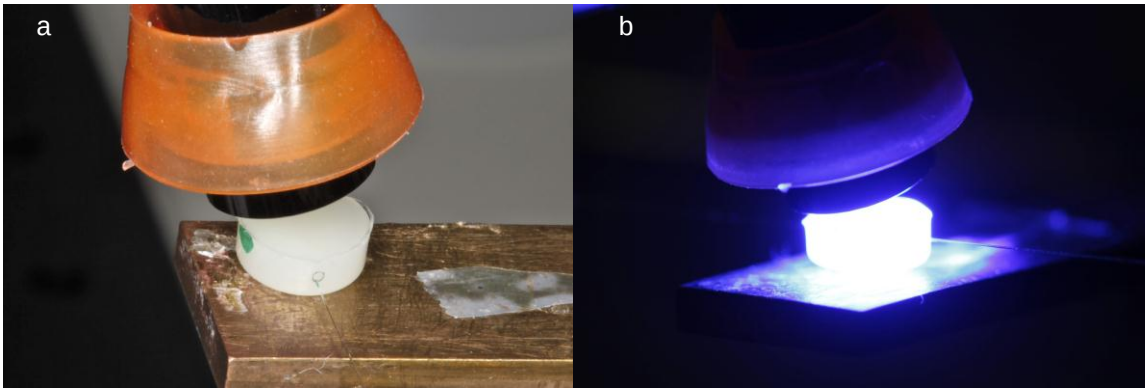

Figure 4a and 4b: Light curing the composite resin.

Additionally, the spectral distribution of the LED light-curing unit used was recorded with a spectrophotometer (Model USB4000 Spectrometer, Ocean Optics Inc, Dunedin, FL, USA).

Results

The temperature rise induced singly by the irradiation with the LED light-curing unit is presented in figure 5. In its low intensity mode a temperature rise of 22,5ºC and 21,6ºC was reached according the two irradiation periods.

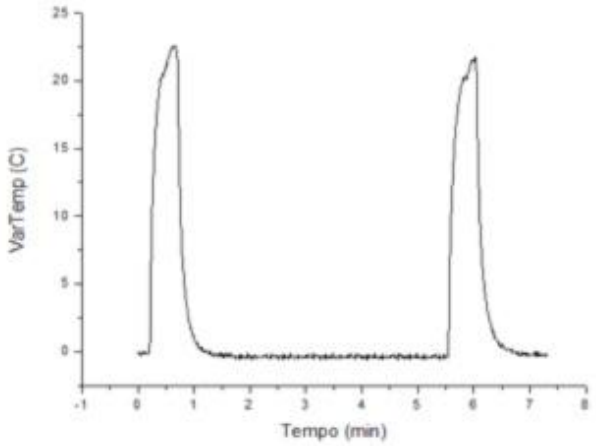

Figure 5: Graphic representation of temperature rise induced solely by the LED light-curing unit.

Thermal characterization of composite resins during light curing is shown in figure 6 For Esthet• X® HD temperature rised to 40,6ºC and 20,6ºC for the 1st and 2nd irradiation period, respectively. SDR™ ascended to 45,6ºC and 11,6ºC for the same periods.

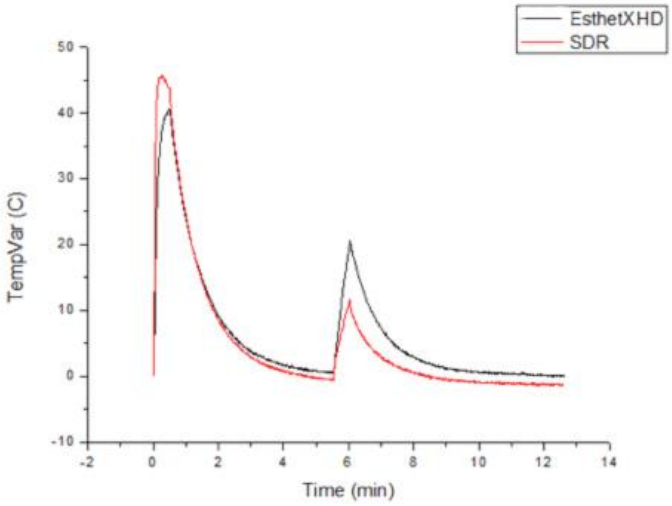

Figure 6: Graphic representation of thermal characterization of SDR™ (red line) and Esthet• X® HD (black line) samples.

Shrinkage strain induced by composite resins polymerization during the light curing process is shown in figures 7a and 7b. Esthet• X® HD and SDR™ presented a final polymerization strain around -4263 μƐ and -4167 μƐ, respectively. A slight initial expansion peak was observed for both composites and irradiation periods.

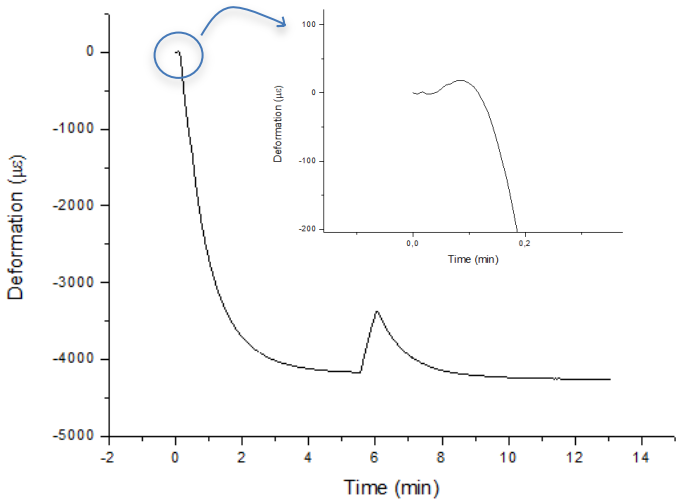

Figure 7a: Graphic representation of polymerization strain of Esthet• X® HD. The identified magnification of the chart details the slightest expansion peak at the beginning of composite light curing.

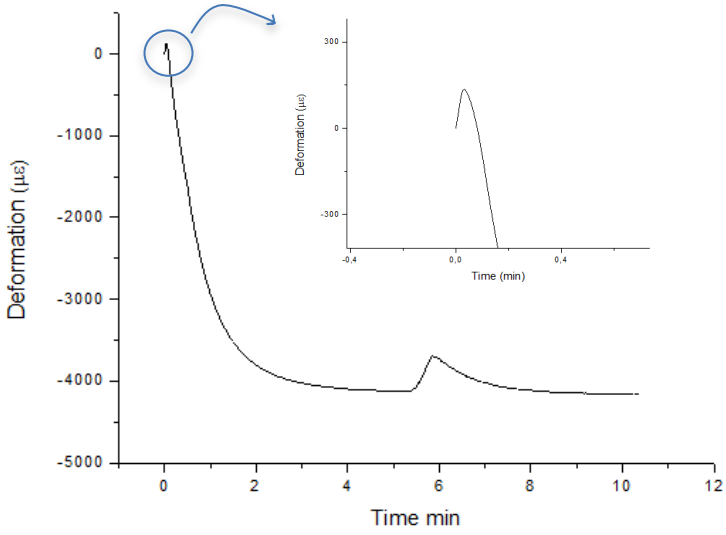

Figure 7b: Graphic representation of polymerization strain of SDR™. The identified magnification of the chart details the slightest expansion peak at the beginning of composite light curing.

Comparison between SDR™ and Esthet• X® HD showed no significant differences in their behavior concerning strain development (figure 8), except that Esthet• X® HD presented slightly more expansion in the beginning of the second peak.

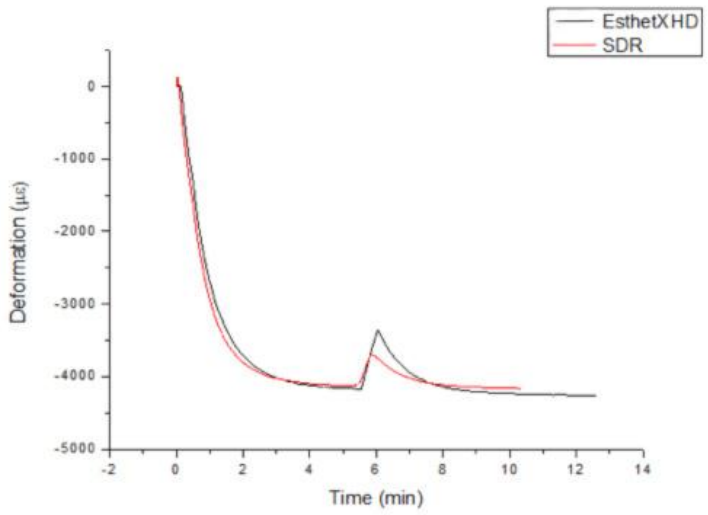

Figure 8**:** Graphic representation of overlapping between Esthet• X® HD and SDR™ behavior strains.

Linear polymerization shrinkage values obtained as a percentage were calculated as follows:

$$LS\% = \frac{\mu\varepsilon}{m} x\ 100$$

Where μƐ is ∆l and m is l. These values are expressed in the same unit (m).

For each composite resin and activation period studied, temperature rise, reported strain (expansion and contraction) as well as linear shrinkage percentage values are summarized in table II.

Table II

	First Peak			Second Peak			
	ºC	με		ºC	με		%
	Temperature	Expansion	Strain	Temperature	Expansion	Strain	LS
Esthet• X ®HD	40,59	17,47	-4171	20,555	810,694	-4263	0,43
SDR™	45,68	133,762	-4134	11,617	436,3497	-4167	0,42

Temperature is expressed in Celsius degrees; expansion and strain are expressed in microstrain units; and linear shrinkage (LS) is expressed in percentage.

Normalized spectral emission of light emitted from LED curing unit used showed the main emission peak at approximately 457 nm (figure 9).

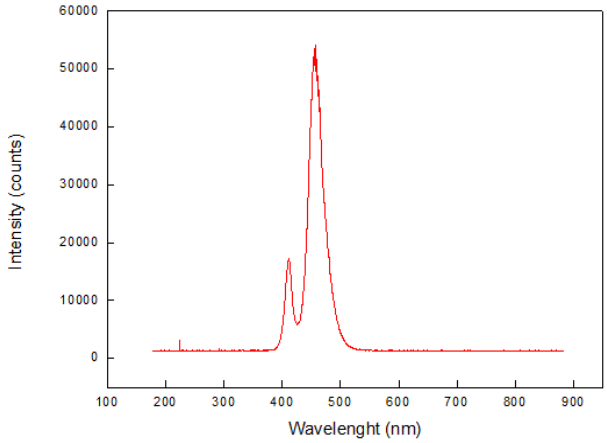

Figure 9: Graphic representation of spectral emission of the light of LED unit Bluephase®

Discussion

Polymerization shrinkage of composite resins results from a molecular re-arrangement in which monomers in the pre-polymerized phase are distanced by van der Walls forces around 0,3 Å. Upon polymerization the breakage of double carbon bonds and subsequent formation of shorter simple covalent carbon-carbon bonds around 0,1 Å, produces cross-linked polymer chains with an inherent resin volumetric loss [5, 18, 34, 39, 52-55]. Shrinkage leads to deformation in the composite resins during curing which being constraint by bonding to cavity walls generates stress [52]. However, the main factors influencing stress development are not only related to the composite volumetric polymerization shrinkage but also with its modulus of elasticity, the adherence quality and the cavity configuration factor (C-factor) [9]. Increasing stress during polymerization may overcome adhesives bond strengths, causing gap formation [9, 56] .

Different strategies to deal with shrinkage stress have been broadly reported and discussed. According to scientific research the use of gold standard adhesive systems along with incremental composite layering procedures and modified polymerization techniques allowing for an extension of the pre-gel phase curing reaction are probably the most important clinical approaches for effective stress relief [27, 57-60]. Polymers visco-elastic behavior determines its flow capacity in the early stages of the curing reaction and, consequently, their modulus of elasticity achieved during polymerization [54]. The relationship between modulus of elasticity and polymerization shrinkage values is a way to predict stress generation at the adhesive interface, since stress is a product of the modulus of elasticity by strain [54].

Bulk filling techniques are undoubtedly more user friendly than the necessary meticulous incremental layering techniques. The entitled stress decreasing resin SDR™ (Dentsply, Konstanz, Germany) was introduced in the market as a flowable composite resin, claiming that it would allow for a 4 mm bulk placement in one layer due to reduced polymerization stress [14] and being mandatorily covered by a 2 mm layer of conventional composite resin [1]. This material is characterized by the incorporation of a polymerization modulator that when interacts with the photoinitiator (canforoquinone) can control kinetics polymerization, delaying the gel point, slowing the rate of polymerization and E-modulus development as well as reducing polymer cross-linking and, consequently, shrinkage stress[61, 62].

Many scientific papers published have focused on different approaches to assess composite polymerization shrinkage. However, the heterogeneity of methodologies along with the fact that shrinkage values significantly depends on the method used to measure it,

limits direct comparisons between reported results [26, 54]. The FBG sensor method for measuring polymerization shrinkage in a real-time recording manner has been described in previous publications that revealed results consistent with the present study, although different composite resins were evaluated [43-45]. Linear polymerization shrinkage of 0,32% for the hybrid composite resin Filtek Z250 and 0,15% for Z100, assessed by FBG sensors, were pointed out by and Anttila et al [44] and Milczewski et al [43], respectively. These authors also suggested that shrinkage values obtained using FBG sensors can be compared to those obtained by using the strain gauge method that revealed a linear shrinkage of 0,55% for Filtek Z250 and 0,12% for Z100 [63, 64]. Nevertheless, strain gauge only records dimensional changes after the material has obtained sufficient elastic rigidity to transfer the shrinkage stresses, therefore only the post-gel shrinkage [26].

Considering the composite resins evaluated in our study we could not found differences between their linear polymerization shrinkage behaviors. As shown in the literature, polymerization shrinkage is a predominantly resin matrix property since it primarily depends on the degree of conversion of monomers [2, 65]. Likewise, monomer composition of composite resins should be carefully analyzed [66]. On the other hand, the increase in the filler fraction incorporated in the resin matrix of a composite resin usually leads to a decrease in its polymerization shrinkage, for reducing its overall matrix content. For the composite resins studied and considering filler fraction by volume, SDR™ contains 45% of inorganic filler compared to the 60% filler volume related to Esthet•X®HD. In what concerns resin matrix composition, both composite resins are mainly based on a high molecular weight urethane modified BisGMA, containing fewer C=C double bond per molecule, which contributes to diminish its polymerization shrinkage, but also diluent monomers like TEGDMA are present. This monomer raises the mobility of molecules during polymerization, increasing their degree of conversion and, consequently polymerization shrinkage [67, 68]. Nevertheless, the novel SDR™ resin technology comprises a unique combination in which a polymerization modulator is chemically embedded in the center of the polymerizable resin backbone of the SDR™ resin monomer. The high molecular weight and the conformational flexibility around the centered modulator impart optimized flexibility to the network structure to SDR™, allowing for a distinct visco-elastic behavior in which this composite resin is able to dissipate more energy and store less when stress is induced during polymerization [62]. This last point may explain why the flowable resin SDR shrinks equally to the more filled microhybrid composite Esthet• X® HD studied.

Previous studies showed a volumetric polymerization shrinkage for Esthet•X™ between 2 and 3% [69-71] while SDR™ revealed values only slightly higher among 3,1% [1] and 3,5% [62]. Limited research is available for the formulation respecting Esthet• X® HD,

nevertheless its major innovation in respect to the more antique Esthet•X™ lies on the filler particle distribution and size which essentially provides better polishing characteristics [71]. No further methods assessing polymerization shrinkage and allowing comparison between those composite resins could be found in literature.

Besides the patent polymerization shrinkage, a slight initial expansion peak was observed for both composite resins on irradiation periods studied. This event was also pointed out by other researchers [43, 44]. During polymerization reaction, the polymer releases bond dissociation energy [72]. Furthermore, absorption of light also increases its temperature [44]. Exothermic polymerization process and absorption of curing light heat can be responsible for the initial expansion peaks. When polymerization shrinkage exceeds thermal expansion, fast overall material shrinking takes place, evidenced by a sharp increase contraction strain [43, 44].

Some drawbacks can be pointed out to the methodology employed in this study concerning FBG sensors. Special caution should be attained due to cross-sensitivity to both strain and temperature, which requires specific techniques to compensate temperature, particularly, by measuring the temperature individually in order to compensate its effect on strain value [43, 44, 46, 51]. Other disadvantage consists on the fiber inherent fragility, which difficult composite placement around it without causing its breakage, particularly in the case of non-flowable composites. Apparently, composite resins adhere relatively easily to the fiber's surface without requiring any pre-treatment. However, there is a lack of research data concerning the effect of some surface fiber pre-treatment on hypothetical interfacial link between the composite resin and the fiber.

In spite of its slightly more expensiveness, FBG sensor is one of the optical methods most commonly used to assess strain. It can measure both linear polymerization shrinkage and expansion of dental materials [44]. Therefore, this method has not only the ability to characterize traditional and new developed formulations of different kind of dental materials, but also the potentiality to evaluate dimensional changes related to cusp deflection and, indirectly to assess the effectiveness of different protocols or clinical modifiable variables that can imply for shrinkage stress management.

Conclusions

The optical fiber Bragg grating sensors can be used to evaluate linear polymerization shrinkage of dental composites with clear advantages to assess the evolution of composite contraction in real time during all polymerization reaction.

Although this study indicated good reliability for the use of FBG sensor as method for determining linear polymerization shrinkage, it should be advocated that more research is necessary concerning composite-fiber interface behavior and other biomechanical dental applications.

Acknowledgments

The authors acknowledge the professional and technical support received from Instituto de Telecomunicações - Pólo de Aveiro.

References

1. Burgess J, Cakir D. Comparative properties of low-shrinkage composite resins. Compend Contin Educ Dent 2010;31 Spec No 2:10-5.
2. Braga RR, Ferracane JL. Alternatives in polymerization contraction stress management. Crit Rev Oral Biol Med 2004;15(3):176-84.
3. Lim BS, Ferracane JL, Sakaguchi RL, Condon JR. Reduction of polymerization contraction stress for dental composites by two-step light-activation. Dent Mater 2002;18(6):436-44.
4. Tantbirojn D, Pfeifer CS, Braga RR, Versluis A. Do low-shrink composites reduce polymerization shrinkage effects? J Dent Res 2011;90(5):596-601.
5. Soh MS, Yap AU, Sellinger A. Physicomechanical evaluation of low-shrinkage dental nanocomposites based on silsesquioxane cores. Eur J Oral Sci 2007;115(3):230-8.
6. Brunthaler A, Konig F, Lucas T, Sperr W, Schedle A. Longevity of direct resin composite restorations in posterior teeth. Clin Oral Investig 2003;7(2):63-70.
7. Tantbirojn D, Versluis A, Pintado MR, DeLong R, Douglas WH. Tooth deformation patterns in molars after composite restoration. Dent Mater 2004;20(6):535-42.
8. Papadogiannis D, Tolidis K, Lakes R, Papadogiannis Y. Viscoelastic properties of low-shrinking composite resins compared to packable composite resins. Dent Mater J 2011;30(3):350-7.
9. Peutzfeldt A, Asmussen E. Determinants of in vitro gap formation of resin composites. J Dent 2004;32(2):109-15.
10. Ferracane JL. Buonocore Lecture. Placing dental composites--a stressful experience. Oper Dent 2008;33(3):247-57.
11. Ferracane JL. Resin composite--state of the art. Dent Mater 2011;27(1):29-38.
12. Klautau EB, Carneiro KK, Lobato MF, Machado SM, Silva e Souza MH, Jr. Low shrinkage composite resins: influence on sealing ability in unfavorable C-factor cavities. Braz Oral Res 2011;25(1):5-12.
13. Umer F, Naz F, Khan FR. An in vitro evaluation of microleakage in class V preparations restored with Hybrid versus Silorane composites. J Conserv Dent 2011;14(2):103-7.
14. Ilie N, Hickel R. Investigations on a methacrylate-based flowable composite based on the SDR technology. Dent Mater 2011;27(4):348-55.
15. Duarte S, Jr., Botta AC, Phark JH, Sadan A. Selected mechanical and physical properties and clinical application of a new low-shrinkage composite restoration. Quintessence Int 2009;40(8):631-8.

16. Meira JB, Braga RR, Ballester RY, Tanaka CB, Versluis A. Understanding contradictory data in contraction stress tests. J Dent Res 2011;90(3):365-70.
17. Leprince J, Palin WM, Mullier T, Devaux J, Vreven J, Leloup G. Investigating filler morphology and mechanical properties of new low-shrinkage resin composite types. J Oral Rehabil 2010;37(5):364-76.
18. Dewaele M, Truffier-Boutry D, Devaux J, Leloup G. Volume contraction in photocured dental resins: the shrinkage-conversion relationship revisited. Dent Mater 2006;22(4):359-65.
19. Mahmoud SH, El-Embaby AE, AbdAllah AM, Hamama HH. Two-year clinical evaluation of ormocer, nanohybrid and nanofill composite restorative systems in posterior teeth. J Adhes Dent 2008;10(4):315-22.
20. Weinmann W, Thalacker C, Guggenberger R. Siloranes in dental composites. Dent Mater 2005;21(1):68-74.
21. Ilie N, Jelen E, Clementino-Luedemann T, Hickel R. Low-shrinkage composite for dental application. Dent Mater J 2007;26(2):149-55.
22. Kleverlaan CJ, Feilzer AJ. Polymerization shrinkage and contraction stress of dental resin composites. Dent Mater 2005;21(12):1150-7.
23. de Melo Monteiro GQ, Montes MA, Rolim TV, de Oliveira Mota CC, de Barros Correia Kyotoku B, Gomes AS, et al. Alternative methods for determining shrinkage in restorative resin composites. Dent Mater 2011;27(8):e176-85.
24. Schneider LF, Cavalcante LM, Silikas N. Shrinkage Stresses Generated during Resin-Composite Applications: A Review. J Dent Biomech 2010;2010.
25. Kim SH, Watts DC. Polymerization shrinkage-strain kinetics of temporary crown and bridge materials. Dent Mater 2004;20(1):88-95.
26. Sakaguchi RL, Wiltbank BD, Shah NC. Critical configuration analysis of four methods for measuring polymerization shrinkage strain of composites. Dent Mater 2004;20(4):388-96.
27. Davidson CL, Feilzer AJ. Polymerization shrinkage and polymerization shrinkage stress in polymer-based restoratives. J Dent 1997;25(6):435-40.
28. Sakaguchi RL, Versluis A, Douglas WH. Analysis of strain gage method for measurement of post-gel shrinkage in resin composites. Dent Mater 1997;13(4):233-9.
29. Boaro LC, Goncalves F, Guimaraes TC, Ferracane JL, Versluis A, Braga RR. Polymerization stress, shrinkage and elastic modulus of current low-shrinkage restorative composites. Dent Mater 2010;26(12):1144-50.
30. Ilie N, Hickel R. Silorane-based dental composite: behavior and abilities. Dent Mater J 2006;25(3):445-54.

31. Ausiello P, Apicella A, Davidson CL, Rengo S. 3D-finite element analyses of cusp movements in a human upper premolar, restored with adhesive resin-based composites. J Biomech 2001;34(10):1269-77.
32. Versluis A, Tantbirojn D, Pintado MR, DeLong R, Douglas WH. Residual shrinkage stress distributions in molars after composite restoration. Dent Mater 2004;20(6):554-64.
33. Versluis A, Tantbirojn D, Douglas WH. Do dental composites always shrink toward the light? J Dent Res 1998;77(6):1435-45.
34. Gustavo Arenas SN, Claudia Vallo, Ricardo Duchowicz. Polymerization shrinkage of a dental resin composite determined by a fiber optic Fizeau interferometer. Optics Communications 2007;271:581-86.
35. Darshil U. Shah PJS. Evaluation of cure shrinkage measurement techniques for thermosetting resins. Polymer Testing 2010;29:629-39.
36. Amore R, Pagani C, Youssef MN, Anauate Netto C, Lewgoy HR. Polymerization shrinkage evaluation of three packable composite resins using a gas pycnometer. Pesqui Odontol Bras 2003;17(3):273-7.
37. Cho E, Sadr A, Inai N, Tagami J. Evaluation of resin composite polymerization by three dimensional micro-CT imaging and nanoindentation. Dent Mater 2011;27(11):1070-8.
38. Tiba A, Charlton DG, Vandewalle KS, Ragain JC, Jr. Comparison of two video-imaging instruments for measuring volumetric shrinkage of dental resin composites. J Dent 2005;33(9):757-63.
39. Lee IB, Cho BH, Son HH, Um CM. A new method to measure the polymerization shrinkage kinetics of light cured composites. J Oral Rehabil 2005;32(4):304-14.
40. Chiang YC, Rosch P, Dabanoglu A, Lin CP, Hickel R, Kunzelmann KH. Polymerization composite shrinkage evaluation with 3D deformation analysis from microCT images. Dent Mater 2010;26(3):223-31.
41. Zeiger DN, Sun J, Schumacher GE, Lin-Gibson S. Evaluation of dental composite shrinkage and leakage in extracted teeth using X-ray microcomputed tomography. Dent Mater 2009;25(10):1213-20.
42. Sun J, Lin-Gibson S. X-ray microcomputed tomography for measuring polymerization shrinkage of polymeric dental composites. Dent Mater 2008;24(2):228-34.
43. Milczewski MS, Silva JC, Paterno AS, Kuller F, Kalinowski HJ. Measurement of composite shrinkage using a fibre optic Bragg grating sensor. J Biomater Sci Polym Ed 2007;18(4):383-92.
44. Anttila EJ, Krintila OH, Laurila TK, Lassila LV, Vallittu PK, Hernberg RG. Evaluation of polymerization shrinkage and hydroscopic expansion of fiber-reinforced

biocomposites using optical fiber Bragg grating sensors. Dent Mater 2008;24(12):1720-7.

45. Quintero SM, Braga AM, Weber HI, Bruno AC, Araujo JF. A magnetostrictive composite-fiber bragg grating sensor. Sensors (Basel) 2010;10(9):8119-28.
46. Othonos A. Fiber Bragg gratings; 1997.
47. Karthick K SK, Geetha Pyra PR, Shankar S. Polymerization Shrinkage of Composites- A review. JIADS 2011;2(2).
48. Flávia Gonçalves LCB, Jack L. Ferracane, Roberto R. Braga. A comparative evaluation of polymerization stress data obtained with four different mechanical testing systems. Dental Materials 2012;28:680-86.
49. Marchesi G, Breschi L, Antoniolli F, Di Lenarda R, Ferracane J, Cadenaro M. Contraction stress of low-shrinkage composite materials assessed with different testing systems. Dent Mater 2010;26(10):947-53.
50. Jong Woon Kim DGL. Measurement of residual stress in thick composite cylinders by the radial-cut-cylinder-bending method. Composite Structures 2007;77:444-56.
51. Carvalho L, Alberto NJ, Gomes PS, Nogueira RN, Pinto JL, Fernandes MH. In the trail of a new bio-sensor for measuring strain in bone: osteoblastic biocompatibility. Biosens Bioelectron 2011;26(10):4046-52.
52. Alvarez-Gayosso C, Barcelo-Santana F, Guerrero-Ibarra J, Saez-Espinola G, Canseco-Martinez MA. Calculation of contraction rates due to shrinkage in light-cured composites. Dent Mater 2004;20(3):228-35.
53. Van Ende A, De Munck J, Mine A, Lambrechts P, Van Meerbeek B. Does a low-shrinking composite induce less stress at the adhesive interface? Dent Mater 2010;26(3):215-22.
54. Gabriela Queiroz de Melo Monteiro MAJRM. Evaluation of Linear Polymerization Shrinkage, Flexural Strenght and Modulus of Elasticity of Dental Composites. Materials Research 2010;13:51-55.
55. Pereira RA, Araujo PA, Castaneda-Espinosa JC, Mondelli RF. Comparative analysis of the shrinkage stress of composite resins. J Appl Oral Sci 2008;16(1):30-4.
56. Park JW, Ferracane JL. Measuring the residual stress in dental composites using a ring slitting method. Dent Mater 2005;21(9):882-9.
57. Manhart J, Chen H, Hamm G, Hickel R. Buonocore Memorial Lecture. Review of the clinical survival of direct and indirect restorations in posterior teeth of the permanent dentition. Oper Dent 2004;29(5):481-508.
58. Kramer N, Garcia-Godoy F, Reinelt C, Feilzer AJ, Frankenberger R. Nanohybrid vs. fine hybrid composite in extended Class II cavities after six years. Dent Mater 2011;27(5):455-64.

59. Frankenberger R, Lohbauer U, Roggendorf MJ, Naumann M, Taschner M. Selective enamel etching reconsidered: better than etch-and-rinse and self-etch? J Adhes Dent 2008;10(5):339-44.
60. van Dijken JW, Pallesen U. Clinical performance of a hybrid resin composite with and without an intermediate layer of flowable resin composite: a 7-year evaluation. Dent Mater 2011;27(2):150-6.
61. Feilzer AJ, de Gee AJ, Davidson CL. Relaxation of polymerization contraction shear stress by hygroscopic expansion. J Dent Res 1990;69(1):36-9.
62. Dentsply D. SDR Scientific Compendium; 2010.
63. Tezvergil A, Lassila LV, Vallittu PK. The effect of fiber orientation on the polymerization shrinkage strain of fiber-reinforced composites. Dent Mater 2006;22(7):610-6.
64. Emami N, Soderholm KJ, Berglund LA. Effect of light power density variations on bulk curing properties of dental composites. J Dent 2003;31(3):189-96.
65. Spinell T, Schedle A, Watts DC. Polymerization shrinkage kinetics of dimethacrylate resin-cements. Dent Mater 2009;25(8):1058-66.
66. Cadenaro M, Marchesi G, Antoniolli F, Davidson C, De Stefano Dorigo E, Breschi L. Flowability of composites is no guarantee for contraction stress reduction. Dent Mater 2009;25(5):649-54.
67. Ferracane JL, Greener EH. The effect of resin formulation on the degree of conversion and mechanical properties of dental restorative resins. J Biomed Mater Res 1986;20(1):121-31.
68. Anseth KS, Goodner MD, Reil MA, Kannurpatti AR, Newman SM, Bowman CN. The influence of comonomer composition on dimethacrylate resin properties for dental composites. J Dent Res 1996;75(8):1607-12.
69. Lien W, Vandewalle KS. Physical properties of a new silorane-based restorative system. Dent Mater 2010;26(4):337-44.
70. C. ANGELETAKIS CT. Polymerization Shrinkage and Volume Loading of New Microhybrid Composites: Abstract. Annual Meeting and Exhibition of the AADR Orange, CA, USA; 2003.
71. Dentsply D. Esthet X micro matrix restorative scientific compendium. In: DeTrey D, editor. United Kingdom, Hamm Moor Lane, Addlestone, Weybridge, Surrey; 1999.
72. Vallittu PK. Peak temperatures of some prosthetic acrylates on polymerization. Journal of Oral Rehabilitation 1996;23:776-81.